



Computational Analysis on the Effect of Size Cylinder for the Irreversible Process in a Piston-Cylinder System using ICED-ALE Method

Open
Access

Siti Nurul Akmal Yusof¹, Yutaka Asako^{1,*}, Tan Lit Ken¹, Nor Azwadi Che Sidik¹

¹ Department of Mechanical Precision Engineering, Malaysia-Japan International Institute of Technology, University Technology Malaysia, Jalan Sultan Yahya Petra, 54100 Kuala Lumpur, Malaysia

ARTICLE INFO

ABSTRACT

Article history:

Received 3 January 2019

Received in revised form 16 April 2019

Accepted 22 April 2019

Available online 26 April 2019

A numerical analysis for the irreversible process in an adiabatic piston-cylinder system has been conducted. Two-dimensional compressible momentum and energy equations were solved numerically to obtain the state quantities of the system using the laminar flow model. The numerical method is based on the combined Implicit Continuous-fluid Eulerian technique and the Arbitrary-Lagrangian-Eulerian method. The computations were performed for a single compression process with the piston velocity of -10 m/s for the effect of diameter cylinder, D which are 0.02 m, 0.04 m and 0.06 m. We found that, size of the diameter cylinder has an effect to the occurrence of the irreversible process. Increase the size of diameter of the cylinder will result in the increases of the average pressure on the piston surface, p_{ps}/p_{rev} in the cylinder. The average value of p_{ps}/p_{rev} during the compression process for the case of the $D = 0.02$ m, 0.04 m and 0.06 m are 1.00026, 1.00042, and 1.00057, respectively.

Keywords:

Laminar flow, reversible process, diameter cylinder, numerical analysis

Copyright © 2019 PENERBIT AKADEMIA BARU - All rights reserved

1. Introduction

Design of heat engines, energy devices in a power plant and thermo-fluid devices have increased the need for fundamental understanding of thermodynamics for the advance of energy and environmental technologies. A process of a compression or an expansion of a gas in a piston-cylinder system is common in many applications, however an irreversible process is not well understood [1-6]. In thermodynamics, state quantities at a final state in a reversible process can be determined. A reversible process may occur when a system is maintained continuously and thermally at an equilibrium state [7-10]. Therefore, the reversible process is also called a quasi-static or a quasi-equilibrium process [8]. The process is reversible when a piston moves with zero velocity in a piston-cylinder system.

On the other hand, the thermal equilibrium state breaks in the system and the process becomes irreversible when the piston moves with infinite velocity. In general, we cannot determine the state

* Corresponding author.

E-mail address: y.asako@utm.my (Yutaka Asako)

quantities at a final state in an irreversible process [9]. The only exception is a throttling process when a gas or a steam passes through a capillary tube or a porous material. For example, in an adiabatic throttling process, the specific enthalpy at the final state is identical to the specific enthalpy at the initial state. Then, the state quantities at the final state can be determined. This strictly highlighted in a thermodynamic textbook [9] that we can make calculations only for a reversible process. All the processes are no reversible processes. This is because, there is no process in nature that can be conducted in a very slow velocity for maintain the state in equilibrium state.

In our previous study, Yusof *et al.*, [11] performed numerical analysis for irreversible processes in a piston-cylinder system. The computations were performed for a single compression process and a single expansion process with the piston velocities of ± 1 m/s, ± 2 m/s, ± 4 m/s, ± 6 m/s, ± 8 m/s and ± 10 m/s and for cyclic compression and expansion processes with sinusoidal velocity variation. It is found that the piston velocities have effects on the state quantities of the piston-cylinder system and it experienced an irreversible process when the piston moved with a finite velocity. Furthermore, it was concluded that the process can be treated as a polytropic process and the polytropic exponent was approximately equal to the adiabatic exponent, n when the piston velocity was less than ± 10 m/s. In the cyclic process of 10000 rpm, the internal energy increases 0.037 % of the compression work in each cycle. In 2019, Yusof *et al.*, [12] solved the irreversible processes in a piston-cylinder system using turbulent flow. Surprisingly, our results show that the system experienced an irreversible process when the piston moved with a finite sinusoidal velocity, too. The p_{ave}/p_{rev} is greater than unity during 10 completed cyclic processes for all cases considered. The value of p_{ave}/p_{rev} at the end of the first cycle for the cases of $N = 10000$ and 50000 rpm were about 1.00045, and 1.00463, respectively. The value of p_{ave}/p_{rev} at the end of each cycle increased in every cycle for all cases. Both of previous papers were analyzed an irreversible process in piston-cylinder system using a fixed diameter cylinder system, $D = 0.04$ m. Although study have recognized the state quantities of the irreversible process when the piston moved with a finite velocity, research has yet to systematically investigate the effect of the diameter cylinder on the state quantities of the irreversible processes in piston-cylinder system. Apart from that, the influence of the size of diameter on the irreversible process in piston-cylinder system. This is the motivation of the present study to conduct numerical analysis for an irreversible process in a piston-cylinder system.

The objective of this paper is to investigate the effect of the diameter cylinder on the state quantities for the irreversible process in piston-cylinder system. The numerical analysis is performed using the numerical method based on the combined technique of the Implicit Continuous-fluid Eulerian (ICE) technique and the Arbitrary Lagrangian Eulerian (ALE) method proposed by Amsden *et al.*, [13]. The computations were performed for a single compression with constant piston velocities.

2. Methodology

2.1 Numerical Approach

In the current research, the simulation code used is a combined technique of the Implicit Continuous-fluid Eulerian (ICE) technique and the Arbitrary Lagrangian Eulerian (ALE) method (ICED-ALE method) proposed by Amsden *et al.*, [13]. An Implicit Continuous-fluid Eulerian (ICED) technique has been proposed as an approach to solve the Navier-Stokes equations in multidimensional fluid dynamic [14-15] in the late of 70's and 80's. The ICE technique was the first method that removed the Courant stability limitation based on sound wave propagation and it is applicable to be use for all flow speeds with the same stability properties in the limit of zero Mach number. The advantages of these combination techniques of ICED and ALE method are, apart from applicable to flows for all speeds, they have an ability to fix arbitrary confining boundaries. The code was written in FORTRAN

and compiled in GFORTRAN COMPILER using Cygwin64 Terminal. Figure 1 shows the flow chart of ICED-ALE method for this research.

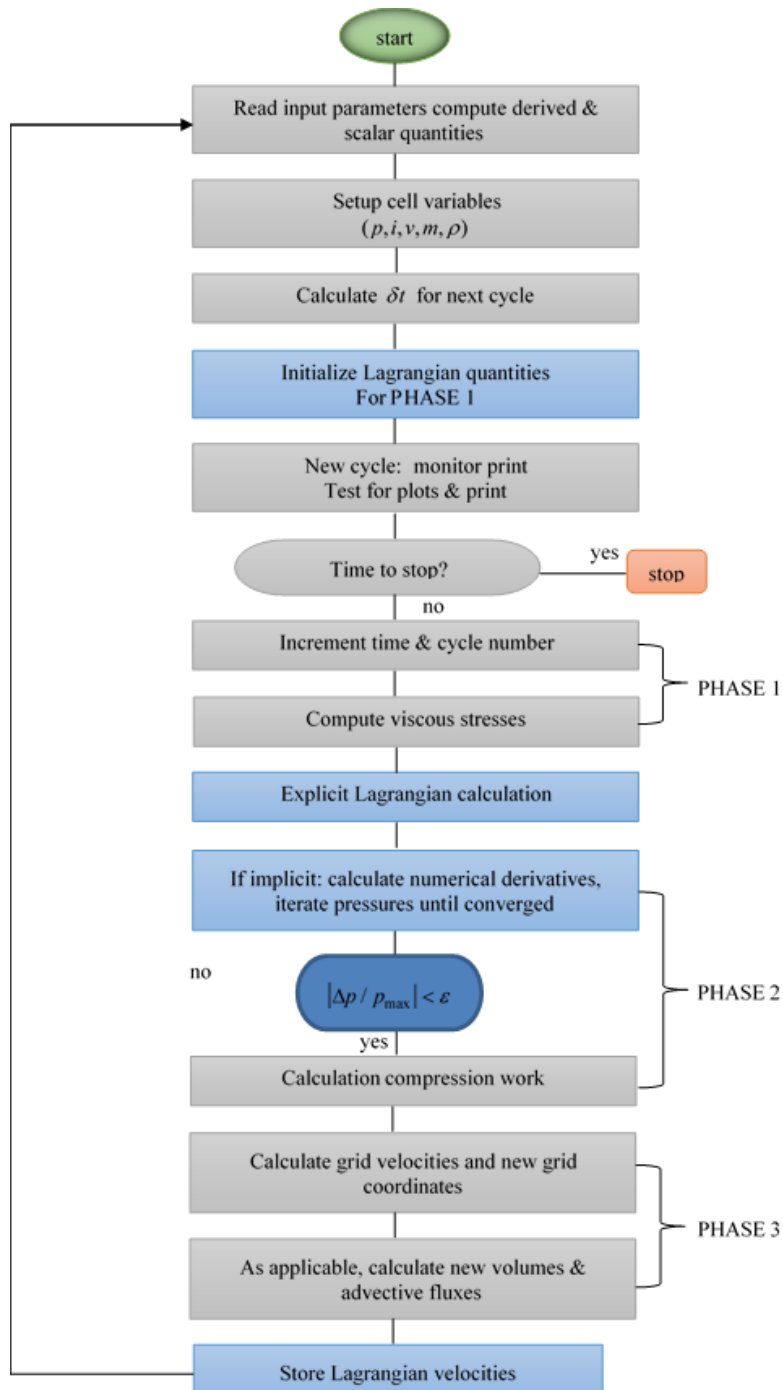


Fig. 1. Flow chart of ICED-ALE method

The computational domain is divided into quadrilateral cells with vertices labelled by integers (i, j) , expressing the column i and row j . The coordinates (x, y) and velocity components (u, v) are defined at the vertices of the cell and fluid variables such as pressures p , specific internal energy I , cell volumes V , and densities ρ or masses M are assigned at the cell centers. Figure 2 shows the assignment of the fluid variables at the cell center.

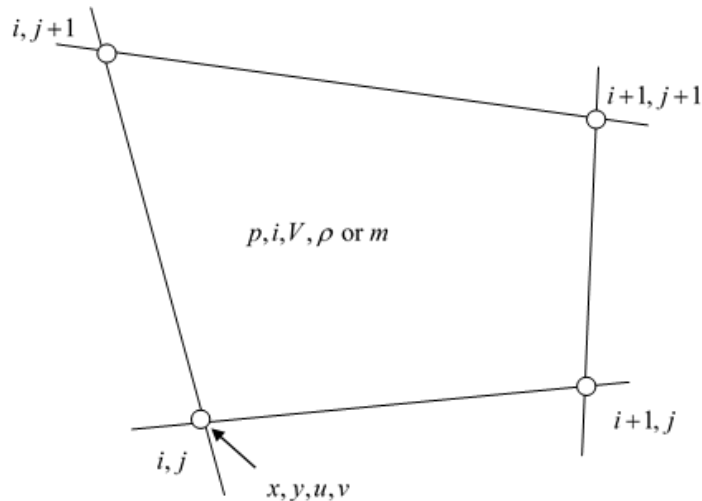


Fig. 2. The assignment of the fluid variables at the cell center

Based on this ICED-ALE method in Figure 1, a flow where the dissipative, transport phenomena of viscosity, mass diffusion and thermal conductivity are neglected. The governing equations to be solved are;

$$\frac{\partial \rho}{\partial t} + \nabla \cdot \rho u = 0 \quad (1)$$

$$\frac{\partial \rho u}{\partial t} + \nabla \cdot \rho u u = -\nabla p + \rho g \quad (2)$$

$$\frac{\partial \rho e}{\partial t} + \nabla \cdot \rho E u = -\nabla \cdot \rho u + \rho g \cdot u \quad (3)$$

Where $e = i + 1/2u^2$, i is the specific internal energy, g is a body acceleration and $p = f(\rho, I)$. Thus, the purpose of this computation are to obtain the fluid variables, pressures p , specific internal energies i , densities ρ , and temperature T at the next time step ($t = \Delta t$). Eq. (1) to Eq. (3) are the continuity, momentum and energy equations for 2D and incompressible fluid flow. These equations need to integrate over a volume which may be moving with an arbitrarily prescribed velocity. The surface of V by surface, S and the outward normal on surface by n are expressed by,

$$\frac{\partial}{\partial t} \int_V \rho dV - \int_S \rho (U - u) \cdot n dS = 0 \quad (4)$$

$$\frac{\partial}{\partial t} \int_V \rho u dV - \int_S \rho u (U - u) \cdot n dS + \int_V \nabla p dV - \int_V \rho g dV = 0 \quad (5)$$

$$\frac{\partial}{\partial t} \int_V \rho e dV - \int_S \rho e (U - u) \cdot n dS + \int_S \nabla p u \cdot n dS - \int_V \rho g \cdot u dV = 0 \quad (6)$$

Where U is the velocity of the surface, S . $U=0$ and $U=u$ when the equations are Eulerian and Lagrangian, respectively. These are the finite difference method which the integration volumes are the cells of a moving mesh as shown in Figure 3. The difference in integration volumes is determined by interpreting fluid densities and energies at cell centers while velocities are interpreted at cell vertices.

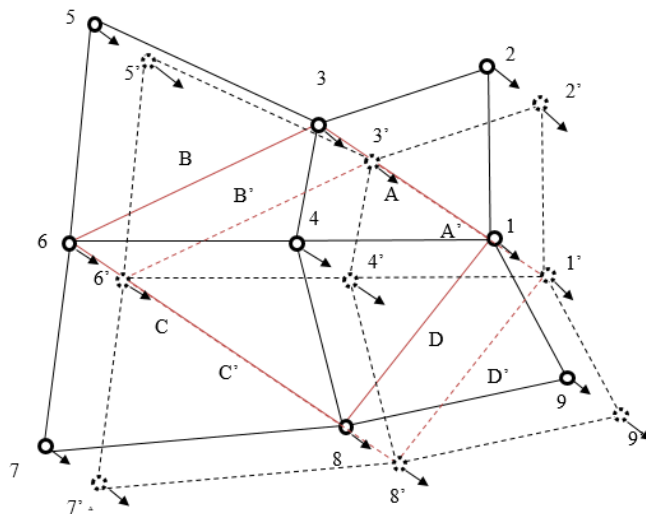


Fig. 3. The dashed line represents the momentum integration volume used for vertex 4. The dotted is the used for specific vertex and cell finite difference equations listed in the text

This ICED-ALE method consists of three phases, which are Phase 1, Phase 2 (first part), Phase 2 (second part), and Phase 3.

Phase 1 is to carry out for an explicit Lagrangian calculation in which the velocities field is updated by the effects of all forces. The velocities rising from this Lagrangian calculation are expressed as u^L and v^L . In this phase, the initializing process is conducted. Once satisfied at the beginning of the calculation, the support quantities include cell volumes, cell total energies and the mass assigned to vertices are automatically updated in the course of a calculation cycle.

Phase 2 (first part) of this method is to obtain a velocity field that has been accelerated with time-advanced pressure gradient. The time-advanced pressures depend upon on the densities and energies acquired when the vertices are moved with these new velocities, denoted as ('') symbol as shown in Figure 3. Thus, due to these are functions of the new pressures, the pressures are defined implicitly and must be specified by iteration. Implicit treatment is responsible to eliminate Courant-like time step restriction to establish computational stability in incompressible flow. Let's considered the desired pressure, p_A^L of cell A from Figure 3 to calculate the implicit problem. A superscript L is representing the time-advanced values, whereas, n is representing the values at the beginning of a cycle. There is the following correlation among the pressure, the density and the specific internal energy of cell A as

$$p_A^L - f(\rho_A^L, i_A^L) = 0 \quad (7)$$

where the new cell density and energy can be defined in terms of their initial values as

$$\rho_A^L = \rho_A^L \frac{V^n}{V^L} \quad (8)$$

Eq. (8) is the Lagrangian expression of the continuity equation.

$$i_A^L = i_A^n + \frac{p_A^n}{\rho_A^n} \left(1 - \frac{V^L}{V^n} \right) \quad (9)$$

where V_A^n is the initial volume of cell A, and V^L is the volume of the cell when the vertices are moving together during time from 0 to Δt which is fluid velocity at Δt .

Now, we will explain the corrected method for the Lagrangian pressure of cell A, p_A^L in Eq. (7). In the case of an ideal gas, Eq. (7) can be rewritten as

$$p = f(\rho, i) = (\gamma - 1)\rho i \quad (10)$$

The residual of the pressure p and the value of the function of f is denoted by s . The residual s can be expressed as

$$s = p - f(\rho, i) (= (\gamma - 1)\rho i) \quad (11)$$

If the density ρ and the specific internal energy i are the converged values, the residual s is 0. However, the residual s is not 0 when the density and the specific internal energy are not converged values. Then substituting p_A^L, ρ_A^L and i_A^L into Eq. (12), the correction value of the pressure is obtained.

$$\Delta p = - \frac{p_A^L - f(\rho_A^L, i_A^L)}{(S_A)} \quad (12)$$

The new guessed value of p_A^L can be obtained by applying a Newton-Raphson iteration into equation Eq. (7) and S_A is a relaxation factor. Compute a pressure change for each cell. The mesh is computed repeatedly until no cell exhibits a pressure change violating the inequality.

$$\left| \frac{\Delta p}{p_{\max}} \right| < \varepsilon \quad (13)$$

where p_{\max} is the actual maximum pressure in the mesh and ε is a selected small number. Typically, ε is order 10^{-3} .

Phase 2 (second part) is responsible to calculate compression work. The final values of u^L, v^L, p^L for Lagrangian velocities and pressures which obtained from the iteration method in the phase 2 (first part) are the new Lagrangian values for the cycles. The pressure works terms is ignored in the first part is now taken account to complete the cycle.

The Lagrangian energy for cell A, E_A^L in Figure 3 is change according to

$$\begin{aligned}
 e_A^L = \tilde{e}_A + \frac{\Delta t}{4M_A} \{ & p_{12}(r_1 + r_2)[(u_1 + u_2)(y_1 - y_2) + (v_1 + v_2)(x_2 - x_1)] \\
 & + p_{23}(r_2 + r_3)[(u_2 + u_3)(y_2 - y_3) + (v_2 + v_3)(x_3 - x_2)] \\
 & + p_{34}(r_3 + r_4)[(u_3 + u_4)(y_3 - y_4) + (v_3 + v_4)(x_4 - x_3)] \\
 & + p_{41}(r_4 + r_1)[(u_4 + u_1)(y_4 - y_1) + (v_4 + v_1)(x_1 - x_4)] \}
 \end{aligned} \tag{14}$$

The pressure along the left edge of cell A are located between vertices 3 and 4. Thus, cell-edge pressure, p_{34} is obtained using the mass weighted method.

$$p_{34} = \frac{M_B p_A^L + M_A p_B^L}{M_A + M_B} \tag{15}$$

Phase 3 of this method is known as rezone and regrid process. Before the rezone calculations are begin, all vertex velocities need to convert to momentum and all cell specific internal energies are converted to total energies so that the rezone are calculated considering of the mass, momentum and energy. For example, if we moved vertex 4 in Figure 3 to the new position at the time 0, the lines connecting it to its neighbors 1, 3, 6 and 8 subtract volumes containing mass and total energy exchange between the adjacent cells (vertex 4 is locates at the center of the control volumes for these vertices). When vertex 4 is moved to the right, the grid line connecting 4 to 3 subtracts volume from cell A and adds to the cell B is

$$\Delta V = \frac{\Delta t}{3} (2r_4 + r_3 [U_4(y_3 - y_4) + V_4(x_4 - x_3)]) \tag{16}$$

where U_4, V_4 are the rezoned velocities specified for the vertex. The mass subtracts from the cell A and adds to the cell B is

$$\Delta M = \frac{1}{2} (\Delta V + \alpha |\Delta V|) \frac{M_A}{V_A} + \frac{1}{2} (\Delta V - \alpha |\Delta V|) \frac{M_B}{V_B} \tag{17}$$

where α is the donor cell weighting factor. When $\alpha = 0$ the flux is centered and $\alpha = 1$ the flux is full donor cell. $\alpha = 1$ is enough due to more stable and accurate.

The energy subtracts from cell A and adds to the cell B is

$$\Delta(Me) = \frac{1}{2} (\Delta V + \alpha |\Delta V|) \frac{M_A e_A}{V_A} + \frac{1}{2} (\Delta V - \alpha |\Delta V|) \frac{M_B e_B}{V_B} \tag{18}$$

Similar formula is computed for the exchange of mass and energy between the other couples of cells surrounding the vertex.

If vertex 4 is located to a new position, it is also need to calculate by considering a momentum exchange between its neighbours 1, 3, 6 and 8. When vertex 4 is moved, the surface connecting vertices 4 and 2 subtracts a volume as,

$$\Delta V = \frac{\Delta t}{3} (2r_4 + r_2 [U_4(y_2 - y_4) + V_4(x_4 - x_2)]) \tag{19}$$

The momentum subtracts from vertex 1 and added to vertex 3. The mass in this volume is $(M_A / V_A) \Delta V$ and the u - momentum it contains is expressed as

$$\Delta(Mu) = \frac{1}{2} \frac{M_A}{V_A} \left[(\Delta V - \alpha |\Delta V|) u_3 + (\Delta V + \alpha |\Delta V|) u_1 \right] \quad (20)$$

Similar formula is computed for the exchange of momentum between the other couples of vertex (3, 6), (6, 8) and (8, 1). Eq. (20) also can be applied for v - momentum with replacing u in the equation. Finally, we obtain the specific internal energy subtracting the kinetic energy from the total energy and the pressure from the specific internal energy and the density.

2.2 Description of the Problem and Conservation Equations

The schematic diagram of the problem under consideration that assumes an insulated piston-cylinder system filled with an ideal gas is shown in Figure 4. The analyses are based on the assumption of a single compression process, a single expansion process and a cyclic compression and expansion processes. The piston is located at the bottom dead center (BDC) at $t \leq 0$ and it begins to compress the gas with constant velocity at $t = 0$. Note that the constant piston velocity was used because we need to investigate fundamentals of reversible and irreversible processes occur during a single compression and expansion processes. The pressure and temperature of the gas increase because of the compression work by the piston. The piston stops when it reaches at the top dead center (TDC). For the case of the expansion process, the piston is located at the TDC at $t \leq 0$. The piston travels with the constant velocity, u_p and it stops when it reaches at the BDC. For the case of cyclic compression and expansion processes, the piston travels with sinusoidal velocity variation. Compressible momentum and energy equations are solved numerically to obtain the pressure and temperature of the gas during the compression or expansion processes. The flow is assumed to be axisymmetric and laminar. The thermo physical properties of the fluid except the density are assumed to be constant. The governing equations can be expressed as follows:

$$\frac{\partial \rho}{\partial t} + \frac{\partial \rho u}{\partial x} + \frac{1}{r} \frac{\partial \rho r v}{\partial r} = 0 \quad (21)$$

$$\frac{\partial \rho u}{\partial t} + \frac{\partial \rho u u}{\partial x} + \frac{1}{r} \frac{\partial \rho r u v}{\partial r} = -\frac{\partial p}{\partial x} + \frac{\partial \tau_{xx}}{\partial x} + \frac{1}{r} \frac{\partial}{\partial r} (r \tau_{rx}) \quad (22)$$

$$\frac{\partial \rho v}{\partial t} + \frac{\partial \rho u v}{\partial x} + \frac{1}{r} \frac{\partial \rho r v v}{\partial r} = -\frac{\partial p}{\partial r} + \frac{\partial \tau_{rx}}{\partial x} + \frac{1}{r} \frac{\partial}{\partial r} (r \tau_{rr}) - \frac{\tau_{\theta\theta}}{r} \quad (23)$$

where

$$\begin{aligned} \tau_{xx} &= \mu \left\{ 2 \frac{\partial u}{\partial x} - \frac{2}{3} \left(\frac{\partial u}{\partial x} + \frac{1}{r} \frac{\partial r v}{\partial r} \right) \right\}, \quad \tau_{xr} = \tau_{rx} = \mu \left(\frac{\partial v}{\partial x} + \frac{\partial u}{\partial r} \right), \\ \tau_{rr} &= \mu \left\{ 2 \frac{\partial v}{\partial r} - \frac{2}{3} \left(\frac{\partial u}{\partial x} + \frac{1}{r} \frac{\partial r v}{\partial r} \right) \right\}, \quad \tau_{\theta\theta} = \mu \left\{ 2 \frac{v}{r} - \frac{2}{3} \left(\frac{\partial u}{\partial x} + \frac{1}{r} \frac{\partial r v}{\partial r} \right) \right\} \end{aligned} \quad (24)$$

$$\frac{\partial \rho i}{\partial t} + \frac{\partial \rho u i}{\partial x} + \frac{1}{r} \frac{\partial \rho r v i}{\partial r} = -p \left(\frac{\partial u}{\partial x} + \frac{1}{r} \frac{\partial r v}{\partial r} \right) + \lambda \left\{ \frac{\partial^2 T}{\partial x^2} + \frac{1}{r} \frac{\partial T}{\partial r} + \frac{\partial^2 T}{\partial r^2} \right\} + \mu \varphi \quad (25)$$

ϕ is dissipation function described as follow

$$\varphi = \left(\frac{\partial u}{\partial r} + \frac{\partial v}{\partial x} \right)^2 + \frac{2}{3} \left(\frac{\partial u}{\partial x} - \frac{\partial v}{\partial r} \right)^2 + \frac{2}{3} \left(\frac{\partial u}{\partial x} - \frac{v}{r} \right)^2 + \frac{2}{3} \left(\frac{\partial v}{\partial r} - \frac{v}{r} \right)^2 \quad (26)$$

The equation of the state for the ideal gas is expressed as

$$i = \frac{1}{\gamma - 1} \frac{p}{\rho} \quad (27)$$

where i is the specific internal energy. At the initial state as the piston stops, the fluid is stationary, and both the temperature and pressure are uniform in the cylinder. Furthermore, with the assumption of no slip boundary condition, the initial and boundary conditions can be expressed as follows:

[Initial conditions]

$$t < 0 \quad : \quad u = v = 0, \quad T = T_i, \quad p = p_i \quad (28)$$

[Boundary conditions]

$$\text{on } r = d/2 \quad : \quad u = v = 0, \quad \partial T / \partial r = 0$$

$$\text{on } r = 0 \quad : \quad \partial u / \partial r = 0, \quad v = 0, \quad \partial T / \partial r = 0$$

$$\text{on piston surface} \quad : \quad u = u_p, \quad v = 0, \quad \partial T / \partial x = 0$$

$$\text{on } x = 0 \quad : \quad u = v = 0, \quad \partial T / \partial x = 0 \quad (29)$$

Attention will now be first focused on the calculation of the average values of the specific internal energy, temperature, density and pressure in the cylinder as follows:

$$i_{ave} = \frac{\int_V \rho i dV}{\int_V \rho dV}, \quad T_{ave} = \frac{i_{ave}}{C_v}, \quad \rho_{ave} = \frac{1}{V} \int_V \rho dV, \quad p_{ave} = (\gamma - 1) \rho_{ave} i_{ave} \quad (30)$$

where i_{ave} is the mass-based average so that mi_{ave} represents the internal energy of the gas in the piston-cylinder device. Note that these average values are a function of time.

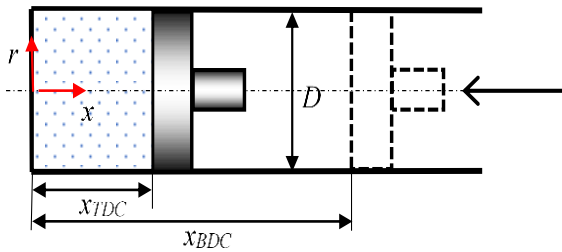


Fig. 4. The schematic diagram of problem

3. Results

The computations were performed for the single compression process. The selected diameter parameters are $D = 0.02$ m, 0.04 and 0.06 m with $x_{TDC} = 0.004$ m and $x_{BDC} = 0.044$ m. The working fluid was air and it was assumed to be an ideal gas. The thermophysical properties of $R = 287$ J/(kg·K), $\gamma = 1.4$, $\mu = 1.862 \times 10^{-5}$ Pa·s and $\lambda = 0.0261$ W/(m·K) were used for the computations. The piston velocity, u_p was ± 10 m/s and fixed for the single compression process. The initial pressure and temperature for the compression case are 1.013×10^5 Pa and 300 K.

The effect of the size diameter of the cylinder system on the pressure and temperature for the compression process are investigated using a piston velocity, -10 m/s. During a reversible adiabatic process, the pressure, p_{rev} and the specific volume, v^* is related by

$$p_{rev} = p_i \left(\frac{v_i^*}{v^*} \right)^\gamma \quad (31)$$

where γ is the specific heat ratio, $\gamma = c_p/c_v$, p_i and v_i^* are the pressure and the specific volume at the initial state. Yusof *et al.*, [16] is presented the details on deriving an expression for the average pressure on the piston surface, p_{ps} in an adiabatic piston-cylinder system during an irreversible compression process with finite piston velocity.

The ratio of the average pressure on the piston surface, p_{ps} , to the pressure of the reversible adiabatic process, p_{ps}/p_{rev} is plotted in Figure 5 and the ratio of the average pressure in the cylinder to the pressure of the reversible process pressure, p_{ave}/p_{rev} , is also plotted in Figure 5. As can be seen from figure, increase the size of diameter cylinder will resulting to the increases of the average pressure on the piston surface, p_{ps}/p_{ave} in the cylinder. The average value of p_{ps}/p_{rev} during the compression process for the case of the $D = 0.02$ m, 0.04 and 0.06 m are 1.00026 , 1.00042 , and 1.00057 , respectively.

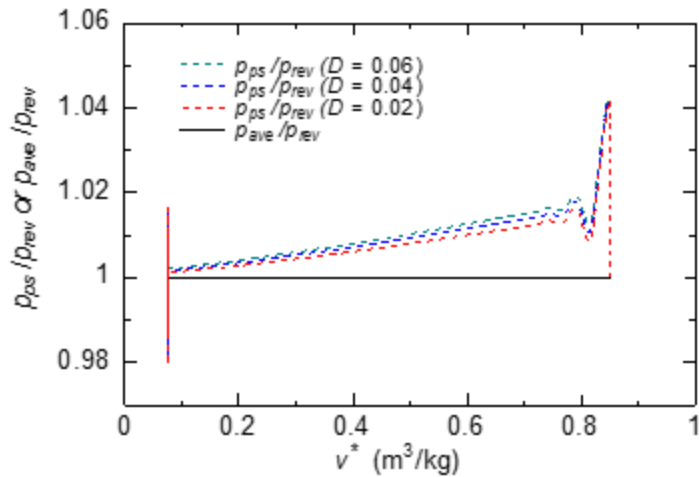


Fig. 5. Pressure ratios, p_{ps}/p_{rev} and p_{ave}/p_{rev} vs v^* of $u_p = -10$ m/s for the size of diameter of 0.02 m, 0.04 m, and 0.06 m

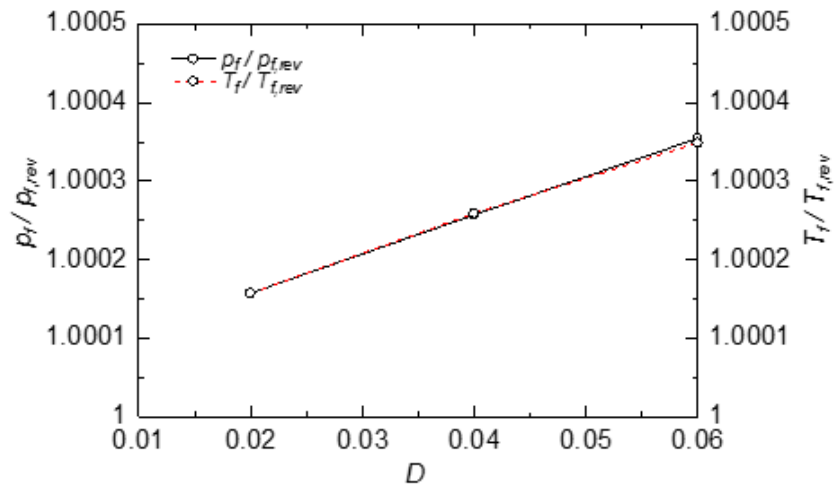


Fig. 6. $p_f/p_{f,rev}$ and $T_f/T_{f,rev}$ vs u_p for compression process

4. Conclusions

In this paper, effect of the diameter cylinder on the state quantities of the irreversible processes in piston-cylinder system has been analysis using ICED-ALE method. The following conclusions are obtained.

1. The system experienced an irreversible process due to the viscous heat generation occurs during the process.
2. The results show that increase of the size of diameter cylinder will resulting to the increases of the average pressure on the piston surface, p_{ps}/p_{ave} in the cylinder.
3. The average value of p_{ps}/p_{rev} during the compression process for the case of the $D = 0.02$ m, 0.04 and 0.06 m are 1.00026, 1.00042, and 1.00057, respectively.

Acknowledgement

The authors would like to express their appreciation to University Technology Malaysia and Takasago Thermal Engineering Co, Ltd., Japan, for providing financial support for this work through Takasago education and research grant (Vote No: R. K130000.7343.4B314).

References

- [1] Anacleto, Joaquim, and J. M. Ferreira. "On the representation of thermodynamic processes." *European Journal of Physics* 36, no. 3 (2015): 035006.
- [2] Anacleto, Joaquim, J. M. Ferreira, and A. A. Soares. "When an adiabatic irreversible expansion or compression becomes reversible." *European Journal of Physics* 30, no. 3 (2009): 487.
- [3] Gislason, Eric A., and Norman C. Craig. "First law of thermodynamics; Irreversible and reversible processes." *Journal of chemical education* 79, no. 2 (2002): 193.
- [4] Plotnikov, L. V., and B. P. Zhilkin. "The gas-dynamic unsteadiness effects on heat transfer in the intake and exhaust systems of piston internal combustion engines." *International Journal of Heat and Mass Transfer* 115 (2017): 1182-1191.
- [5] Sieniutycz, Stanislaw. "Variational setting for reversible and irreversible fluids with heat flow." *International Journal of Heat and Mass Transfer* 51, no. 11-12 (2008): 2665-2675.
- [6] Zhao, Yingru, and Jincan Chen. "An irreversible heat engine model including three typical thermodynamic cycles and their optimum performance analysis." *International Journal of Thermal Sciences* 46, no. 6 (2007): 605-613.
- [7] Norton, John D. "The impossible process: Thermodynamic reversibility." *Studies in History and Philosophy of Science Part B: Studies in History and Philosophy of Modern Physics* 55 (2016): 43-61.
- [8] Guha, Evelyn. *Basic thermodynamics*. Alpha Science Int'l Ltd., 2000.
- [9] Y. Çengel, M.A. Boles, *Thermodynamics: An Engineering Approach*, 2nd edition, McGraw-Hill, New York, 1994.
- [10] Sobel, Michael I. "Kinetic theory derivation of the adiabatic law for ideal gases." *American Journal of Physics* 48, no. 10 (1980): 877-878.
- [11] Yusof, Siti Nurul Akmal, Yutaka Asako, Mohammad Faghri, Lit Ken Tan, and Nor Azwadi bin Che Sidik. "Numerical analysis for irreversible processes in a piston-cylinder system." *International Journal of Heat and Mass Transfer* 124 (2018): 1097-1106.
- [12] Yusof, Siti Nurul Akmal, Yutaka Asako, Mohammad Faghri, Lit Ken Tan, Nor Azwadi bin Che Sidik, and Wan Mohd Arif bin Aziz Japar. "Numerical analysis of irreversible processes in a piston-cylinder system using LB1S turbulence model." *International Journal of Heat and Mass Transfer* 136 (2019): 730-739.
- [13] Amsden, A. A., H. M. Ruppel, and C. W. Hirt. *SALE: A simplified ALE computer program for fluid flow at all speeds*. No. LA-8095. Los Alamos Scientific Lab., NM (USA), 1980.
- [14] Hirt, Cyril W., Anthony A. Amsden, and J. L. Cook. "An arbitrary Lagrangian-Eulerian computing method for all flow speeds." *Journal of computational physics* 14, no. 3 (1974): 227-253.
- [15] Amsden, Anthony A., Peter J. Orourke, and T. Daniel Butler. "KIVA-2: A computer program for chemically reactive flows with sprays." *NASA STI/recon technical report N* 89 (1989).
- [16] Yusof, Siti Nurul Akmal, Yutaka Asako, Tan Lit Ken, and Nor Azwadi Che Sidik. "Piston Surface Pressure of Piston-Cylinder System with Finite Piston Speed." *Journal of Advanced Research in Fluid Mechanics and Thermal Sciences* 44, no.1 (2018): 55-65.